C. -C. Shir

Numerical Investigation of the Atmospheric Dispersion of Stack Effluents

Abstract: This report describes a numerical method based on the best gradient-transfer theory currently available for computing pollutant concentration distributions downwind from a stack. The vertical inhomogeneity of the atmosphere and ground roughness are included in the model. Vertical wind and temperature profiles are calculated numerically from given values of ground roughness and wind speed and relative temperature at stack height. An equation governing the plume from the stack is solved by a finite difference method. The numerical results, compared with several experiments, suggest that ground roughness is an important parameter and that disagreement between different sets of experimental data may be due to different values of this parameter. The effect of wind is found to be small under neutral conditions. The effective mean wind decreases to a minimum value a short distance from the stack and then increases downwind.

Introduction

Methods of estimating atmospheric dispersion have been studied for a long time and have undergone considerable revision because of experimental results. Among the important parameters affecting dispersion are atmospheric stability, ground roughness, and wind speed. Atmospheric stability has been investigated experimentally, but results from different experiments are inconsistent[1]. Very little work has yet been done toward understanding the other two parameters.

This report describes a numerical method used to predict concentration distributions downwind from a stack. Atmospheric stability, ground roughness, wind speed, and vertical inhomogeneity have been considered. The method of analysis is based on the best gradient-transfer theory currently available. Numerical results compared with experiments show that ground roughness is an important parameter; this finding suggests that the disagreement among published dispersion data[2,3] may be due to different ground-roughness conditions at the testing sites. The effect of wind speed is found to be small under conditions of neutral atmospheric stability. Effective mean wind (or mean equivalent wind), which is the optimum wind speed in the plume diffusion model, has previously been regarded as monotonically increasing downwind from the stack. However, the computational results show that, because of ground reflection, the effective mean wind decreases to a minimum value and then increases downwind.

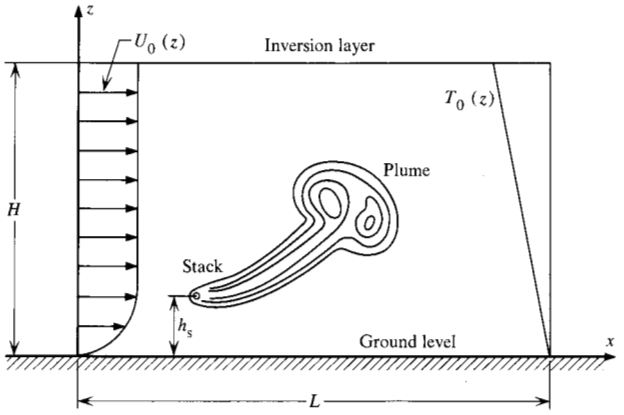

Figure 1 Two-dimensional stack model.

Stack model

• *Configuration and parameters included*

We consider two-dimensional flow in the lower atmosphere bounded below by the ground and above by an inversion layer, as shown in Fig. 1. Vertical variation of wind direction is neglected and the ground is assumed to be horizontally homogeneous. However, vertical variations of wind speed, temperature, and eddy coefficients are included. Special emphasis is given to ground roughness.

At time zero, a stack begins to emit at a steady rate. The spatial and temporal variation of pollutant concentration are computed for times thereafter.

• *Equations and boundary conditions*

The process of plume dispersion can be divided into two parts, viz., plume rise and diffusion caused by atmospheric turbulence. (The appropriate equations have been derived in Ref. 4.) Since the numerical results are to be compared here with observations that are associated only with diffusion, just the concentration equation was integrated. The pollutants are considered to be chemically inert, and the wind and the temperature are assumed to be constant in time and functions of height only. Turbulence was not treated explicitly. The amount of diffusion caused by turbulent air is approximated by an eddy diffusivity coefficient.

The concentration equation is

$$\partial C/\partial t + \mathbf{V}\cdot\nabla C = \nabla\cdot(K_c \nabla C) + Q_c, \tag{1}$$

where C and $\mathbf{V}$ are mean concentration and wind velocity, respectively; K_c is the eddy diffusivity coefficient; and Q_c is the pollutant source strength. Boundary conditions on the concentration are

$$K_c \partial C/\partial z = 0 \text{ at } z = 0 \text{ and } z = H, \tag{2}$$

where H is the height of the inversion layer (mixing depth). The temperature T is prescribed on the boundary surfaces.

When the variation of wind direction is neglected, Eq. (1) is simplified to

$$\frac{\partial C}{\partial t} + U\frac{\partial C}{\partial x} = \frac{\partial}{\partial z}\left(K_c \frac{\partial C}{\partial z}\right) + K_h\left(\frac{\partial^2 C}{\partial x^2} + \frac{\partial^2 C}{\partial y^2}\right) + \overline{Q}_c\,\delta(x, y, z - h_s), \tag{3}$$

where $Q_c = \overline{Q}_c\,\delta(x, y, z)$, $K_c = K_c(z)$ has been assumed, δ is the Dirac delta function, and h_s is the stack height.

Let $\overline{C} = \int_{-\infty}^{\infty} C\,dy$ and assume C to be symmetric in y. Integrating Eq. (3) along y, we have

$$\frac{\partial \overline{C}}{\partial t} + U\frac{\partial \overline{C}}{\partial x} = \frac{\partial}{\partial z}\left(K_c \frac{\partial \overline{C}}{\partial z}\right) + K_c \frac{\partial^2 \overline{C}}{\partial x^2} + \overline{Q}_c\,\delta(x, z - h_s). \tag{4}$$

The horizontal diffusion term on the right can be neglected in comparison with the advection term. The concentrations computed from Eq. (4) are compared with values obtained from Eq. (33), which contains standard deviation (σ_z) values that are frequently published in lieu of the actual concentration data. Values of σ_z are usually obtained from observed ground-level concentrations through Eq. (33) under the assumptions that there is no crosswind and the concentration distribution in that direction is Gaussian. However, a crosswind often exists, and this causes the plume center line to deviate from the straight downwind line, thus introducing some discrepancies between the computed and the observed results at far distances. If the plume rise must be considered, deduction of the information about a plume from a two-dimensional study becomes more complicated, as shown by Langlois[5] (also see the Appendix).

Vertical variation of meteorological parameters

The wind and temperature profiles, ground roughness, stack height, and mixing depth are basic input parameters to the model. However, the upper layer wind and temperature profiles (above 50 m) are difficult to prescribe analytically and field measurements are not always available. For practical purposes, we require only the ground roughness and the wind speed and relative temperature at the top of the stack. From these values, the wind, temperature, and eddy coefficients over the whole layer can be estimated numerically.

• *Theory*

The wind and temperature profiles are determined from planetary boundary layer theory, augmented by certain assumptions described below. The boundary layer is assumed to consist of a lower contact layer ($z \le h$) and an upper transition layer ($h \le z \le H$).

Lower contact layer ($z \le h = 60$ m)

The wind and potential temperature in this layer are computed from the following equations[6]:

$$U = \frac{U_*}{k} f(z; Z_0, U_*, \theta_*) \quad \text{and} \tag{5}$$

$$\theta - \theta_0 = \frac{\theta_*}{k} f(z; Z_0, U_*, \theta_*), \tag{6}$$

where

$$f(z) \equiv f(z; Z_0, U_*, \theta_*) = \ln\left(\frac{z + Z_0}{Z_0}\right)\Phi(S); \tag{7}$$

$$\Phi(S) = \begin{cases} 1 + \alpha S, & S \ge 0; \\ (1 - \alpha S)^{-1}, & S \le 0; \end{cases} \tag{8}$$

$$S = \frac{\sqrt{gz}}{\bar{\theta}}\frac{\theta_*}{U_*}\Big/ \ln\left(\frac{z + Z_0}{Z_0}\right); \tag{9}$$

$$\theta_* = -H_0/\rho C_p U_*; \tag{10}$$

U_* is friction velocity; θ_* is "heat flux" temperature; Z_0 is ground roughness parameter (height); k is von Karman's constant; α is a constant taken as 18; $\Phi(S)$ is a function that depends on atmospheric stability; $\bar{\theta}$ is the average potential temperature; H_0 is the vertical heat flux; and C_p and ρ are the specific heat and density of air, respectively.

Upper transition layer ($h \le z \le H$)

The wind and temperature in this layer cannot be prescribed analytically. To evaluate them numerically one must know the horizontal pressure gradient and the eddy coefficients through the whole boundary layer (up to 1 or 2 km). This much information is seldom available.

For practical purposes, we simply assume that the vertical fluxes of momentum and heat decrease linearly with increasing height. Thus

$$K_v \frac{\partial U}{\partial z} = K_v \frac{\partial U}{\partial z}\bigg|_h \left(\frac{H - mz}{H - mh}\right), \qquad z \ge h; \tag{11}$$

and

$$K_t \frac{\partial \theta}{\partial z} = K_t \frac{\partial \theta}{\partial z}\bigg|_h \left(\frac{H - mz}{H - mh}\right), \qquad z \ge h, \tag{12}$$

where m, a constant determining the decreasing rate of flux, is chosen as $H/(2H - h)$, K_v is the eddy viscosity, and K_t is the eddy conductivity.

With this choice of m, the fluxes at the top of the layer are equal to one half of those at the bottom and decrease to zero inside the inversion layer. Physically, the fluxes should be zero at the base of the inversion layer. The heat flux may even reach zero below the inversion layer. However, the uncertainty of this assumption is covered by the uncertainty of the assumption of linear flux distribution and the fixed height of the mixing layer. Moreover, these assumptions are not critical to the determination of where the maximum ground concentration occurs. The momentum flux is assumed to be positive, i.e., $\partial U/\partial z \ge 0$.

The eddy coefficients are computed from the formula

$$K_v = K_t = l^2 |\partial U/\partial z| \phi(\gamma); \tag{13}$$

also $K_c = K_v \phi(\gamma)$. Here l is the mixing length described as

$$l = \begin{cases} k(z + Z_0), & z \le h'; \\ \dfrac{k(z + Z_0)}{1 + k(z - h')/\lambda}, & h' \le z \le H, \end{cases} \tag{14}$$

and $\phi(\gamma)$ is a function of atmospheric stability.

The mixing length increases linearly near the surface (below $h' = 10$ m) and approaches a limit λ at greater height. Equation (14) is modified from the formula used by Blackadar[7] in order to make l continuous through the whole layer.

The atmospheric stability function is defined by

$$\phi(\gamma) = \begin{cases} 1 - \alpha\gamma, & \gamma \le 0; \\ (1 + \alpha\gamma)^{-1}, & \gamma \ge 0, \end{cases} \tag{15}$$

where

$$\gamma = \frac{\sqrt{gl}}{\bar{\theta}} \frac{\partial \theta/\partial z}{|\partial U/\partial z|}. \tag{16}$$

This is Clayton's formula as used by Estoque[6]. According to Clayton, the formula works well over a wide range of conditions. However, the present study does not confirm this advantage. Use of the Obukhov-Monin length or the bulk Richardson number may be a better approach.

Equation (13) is not necessarily a good assumption. It may be better to use the relation $K_c = K_t = K_v \phi(\gamma)$. However, only K_c is used for computing concentration distributions; K_v and K_t are used only for setting the vertical variation of U and θ. Consequently, the exact form of Eq. (13) may not be important except in strongly stable or unstable cases, and then Clayton's formula may not apply. These latter cases have not been included in our results.

• *Application*

Computation of wind and temperature profiles is not straightforward because U_* and θ_* are unknown quantities. The parameters given are h_s (stack height), U_s (wind speed at stack height), $\theta_s - \theta_0$ (potential temperature at stack height relative to that at ground level), and Z_0 (ground roughness). There are two distinct cases, $h_s \le h$ and $h < h_s \le H$. The computation procedures for each case are described below.

Stack height in the lower layer ($h_s \le h$)

From Eqs. (5) and (6) we have

$$U_s = \frac{U_*}{k} f(h_s), \qquad \text{and} \tag{5'}$$

$$\theta_s - \theta_0 = \frac{\theta_*}{k} f(h_s). \tag{6'}$$

These lead to

$$\frac{\theta_s - \theta_0}{U_s} = \frac{\theta_*}{U_*}. \tag{17}$$

Equations (9) and (17) lead to

$$S_s = \frac{\sqrt{g h_s}}{\bar{\theta}} \left(\frac{\theta_s - \theta_0}{U_s}\right) \Big/ \ln\left(\frac{h_s + Z_0}{Z_0}\right). \tag{9'}$$

From this we compute $f(h_s)$ using (7) and then compute U_* and θ_* using (5') and (6').

Stack height in the upper layer ($h \le h_s \le H$)

First we show that

$$\frac{\theta_s - \theta_0}{U_s} = \frac{\theta_h - \theta_0}{U_h} = \frac{\theta^*}{U^*} \qquad \text{for } h \le h_s. \tag{18}$$

From Eqs. (11) and (13) we obtain

$$l^2 \left(\frac{\partial U}{\partial z}\right)^2 \phi(\gamma) = l_h^2 \frac{\partial U}{\partial z}\bigg|_h^2 \phi(\gamma_h) \left(\frac{H - mz}{H - mh}\right) \tag{19}$$

for $h \leq z \leq H$, where subscript h denotes evaluation at $z = h$. Since $\partial U/\partial z$ is positive, Eq. (19) can be rewritten as

$$\frac{\partial U}{\partial z} = \left.\frac{\partial U}{\partial z}\right|_h I(z), \tag{20}$$

where $I(z)$ is a positive-valued function defined by

$$I(z) = \frac{l_h}{l}\left[\frac{\phi(\gamma_h)(H - mz)}{\phi(\gamma)(H - mh)}\right]^{1/2}. \tag{21}$$

Thus

$$U = U_h + \left.\frac{\partial U}{\partial z}\right|_h \int_h^z I(z')\, dz'. \tag{22}$$

In particular,

$$U_s = U_h + \left.\frac{\partial U}{\partial z}\right|_h \int_h^{h_s} I(z')\, dz'. \tag{23}$$

Similarly, Eqs. (12) and (13) lead to

$$\frac{\partial \theta}{\partial z} = \left.\frac{\partial \theta}{\partial z}\right|_h I(z). \tag{24}$$

Integrating Eq. (24) we obtain the generic and specific results

$$\theta - \theta_0 = \theta_h - \theta_0 + \left.\frac{\partial \theta}{\partial z}\right|_h \int_h^z I(z')\, dz' \tag{25}$$

and

$$\theta_s - \theta_0 = \theta_h - \theta_0 + \left.\frac{\partial \theta}{\partial z}\right|_h \int_h^{h_s} I(z')\, dz'. \tag{26}$$

However,

$$\left.\frac{\partial U}{\partial z}\right|_h = \frac{U_*}{k} f'(h) \quad \text{and} \quad \left.\frac{\partial \theta}{\partial z}\right|_h = \frac{\theta_*}{k} f'(h), \tag{27}$$

so that

$$\left.\frac{\partial \theta}{\partial z}\right|_h = \left.\frac{\partial U}{\partial z}\right|_h \frac{\theta_*}{U_*}. \tag{28}$$

Also, from Eqs. (5) and (6),

$$\theta_h - \theta_0 = U_h \frac{\theta_*}{U_*}. \tag{29}$$

Substituting (28) and (29) into (26) and comparing the result with (23), we establish the intended result (18).

Next, we observe from Eqs. (16), (20), (24), and (28) that for $h \leq z \leq H$,

$$\gamma = \frac{\sqrt{gl}}{\bar{\theta}} \frac{\theta_*}{U_*}. \tag{30}$$

Finally, with the relations

$$U_h = \frac{U_*}{k} f(h) \quad \text{and} \quad \left.\frac{\partial U}{\partial z}\right|_h = \frac{U_*}{k} f'(h), \tag{31}$$

we can rewrite Eqs. (22), (23), (25), and (26):

$$U = U_h\left[1 + \frac{f'(h)}{f(h)} \int_h^z I(z')\, dz'\right]; \tag{22'}$$

$$U_s = U_h\left[1 + \frac{f'(h)}{f(h)} \int_h^{h_s} I(z')\, dz'\right]; \tag{23'}$$

$$\theta - \theta_0 = (\theta_h - \theta_0)\left[1 + \frac{f'(h)}{f(h)} \int_h^z I(z')\, dz'\right]; \tag{25'}$$

and

$$\theta_s - \theta_0 = (\theta_h - \theta_0)\left[1 + \frac{f'(h)}{f(h)} \int_h^{h_s} I(z')\, dz'\right]. \tag{26'}$$

In summary, the procedure for determining the initial conditions is as follows:

1. Begin with U_s, $\theta_s - \theta_0$, h_s and Z_0 as input data.
2. Calculate θ_*/U_* from Eq. (18).
3. Calculate U_h from Eq. (23′) and $\theta_h - \theta_0$ from Eq. (26′), with Eq. (30) for γ in the definition of $I(z)$.
4. Calculate U_* and θ_* from Eq. (31) and the results of step 2.
5. Compute U and θ in the lower layer from Eqs. (5) and (6) and in the upper layer from Eqs. (22′) and (25′).
6. Calculate K_v and K_t from Eq. (13). [The eddy diffusivity K_c is taken as $K_v\,\phi(\gamma)$.]

Analysis

At time zero the stack begins to emit pollutant at a constant rate Q_c. The governing equations are solved by a finite difference method, the details of which are given in Ref. 4. The pollutant concentration at each grid point is computed at successive time steps in a forward moving procedure, starting from initial conditions derived by the procedure set out in the previous section.

• *Parameters*

In the present study we investigate three parameters that can influence the dispersion of contaminants, viz., atmospheric stability, ground roughness, and wind speed.

Many investigations of the effect of atmospheric stability on dispersion have been documented, but the results are quite diverse. Moreover, the comparison between theory and experiment is difficult because different measures of atmospheric stability are used. In theoretical work, the stability is usually characterized by the Richardson number or the Obukhov-Monin length. In experiments, the stability category is denoted by insolation, cloud cover, or wind gustiness. This ambiguity is not the main problem, however. We show that specifying the atmospheric stability is not enough; the behavior of stack effluents is also influenced by ground roughness and wind speed.

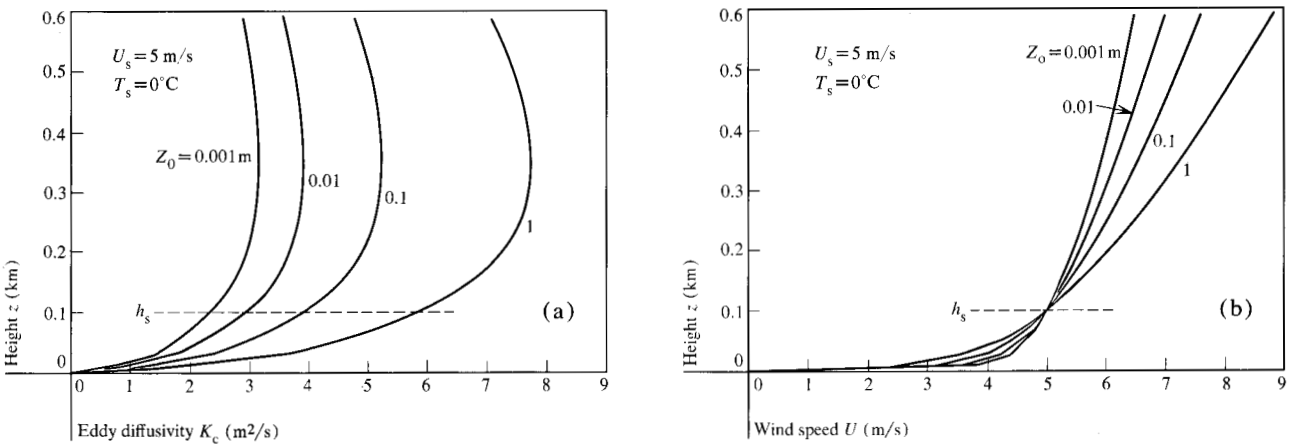

Figure 2 Vertical variation of (a) eddy diffusivity and (b) wind speed with ground roughness.

Ground roughness is a parameter that is neglected in the usual diffusion approach. Its effects have been realized but no investigation has been made. The computations reported here show that ground roughness is as important as the atmospheric stability. Our results show that the differences among experiments could be due to differing ground roughness at the experimental sites.

In a uniform wind field the absolute concentration $\overline{C}$ is inversely proportional to wind speed. Hence, the relative concentration $\overline{C}\,\overline{U}/Q_c$ is independent of the wind speed. However, it has not previously been clear that the relative concentration should depend upon $\overline{U}$ in a nonuniform wind field. In this study, the dependence upon $\overline{U}$ is found to be small for a nonuniform wind field in a neutrally stable atmosphere.

• *Ground-level concentration*

Our computation field is the two-dimensional equivalent of an infinite-line stack in a uniform cross-wind field. When the cross wind is small, the two-dimensional result can be compared with the cross-wind integration of three-dimensional values. Since most experiments determine vertical and horizontal deviations (σ_z, σ_y) from the Gaussian plume formula, this integration is straightforward.

The ground concentration in the Gaussian plume model is described by the formulas

$$C = \frac{Q_c}{\overline{U}\,\sigma_y\,\sigma_z\pi} \exp\left[-\frac{1}{2}\left(\frac{h_s^2}{\sigma_z^2} + \frac{y^2}{\sigma_y^2}\right)\right] \quad \text{and} \tag{32}$$

$$\overline{C} = \int_{-\infty}^{\infty} C\,dy = \sqrt{\frac{2}{\pi}}\,\frac{Q_c}{\overline{U}\sigma_z} \exp\left[-\frac{1}{2}\left(\frac{h_s}{\sigma_z}\right)^2\right]. \tag{33}$$

The maximum value of $\overline{C}\,\overline{U}/Q_c$ is given by

$$\max\left(\frac{\overline{C}\,\overline{U}}{Q_c}\right) = \sqrt{\frac{2}{\pi e}}\,\frac{1}{h_s} \quad \text{at } x = x_m, \tag{34}$$

where $\sigma_z(x_m) = h_s$.

• *Effective mean wind*

In the usual diffusion calculation of pollutant concentration the wind field is assumed to be uniform, but in the lower atmosphere, the wind strength actually increases significantly with height. A proper method of choosing the parameter $\overline{U}$, which is usually interpreted as mean wind speed in Eqs. (32) and (33), is important. Smith and Singer[8] pointed out that the predicted concentration can vary by a factor of three at medium distance (5 km) downwind, depending on the way $\overline{U}$ is selected. They suggested that the optimum wind speed for estimating dispersion should be the effective mean wind (mean equivalent wind) defined by

$$\overline{U}(x) = \frac{\int_0^H U(z')\,\overline{C}(x,z')\,dz'}{\int_0^H \overline{C}(x,z')\,dz'}. \tag{35}$$

Smith and Singer also derived a simple formula for estimating the effective mean wind. According to their formula, the effective mean wind is monotonically increasing as is usually assumed. In this study, we evaluate $\overline{U}$ in Eq. (35) numerically. The results discussed in the next section show that the effective mean wind decreases to a minimum value due to ground reflection and then increases downwind. Singer (personal communication) anticipated that this might be the case for an elevated source. The Smith and Singer formula, which is derived from a surface source, may not apply to an elevated source. However, it may give an approximate estimate at distances far downwind where the vertical concentration distribution is nearly uniform.

Results

• *Ground roughness*

In Fig. 2(a) the ground roughness parameter ranges from 0.001 to 1 m and $T_s = \theta_s - \theta_0 = 0$, which is the condition

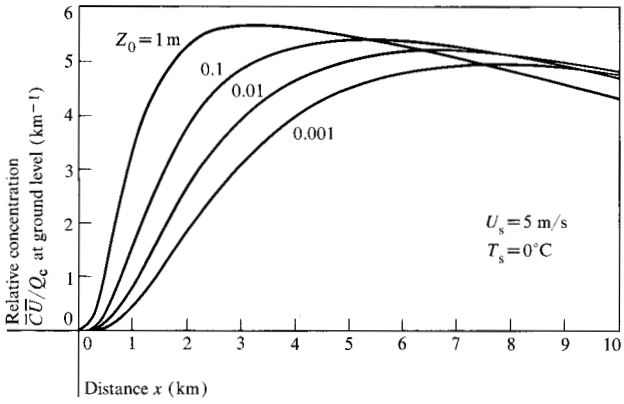

Figure 3 Horizontal variation of relative ground-level pollutant concentration with ground roughness.

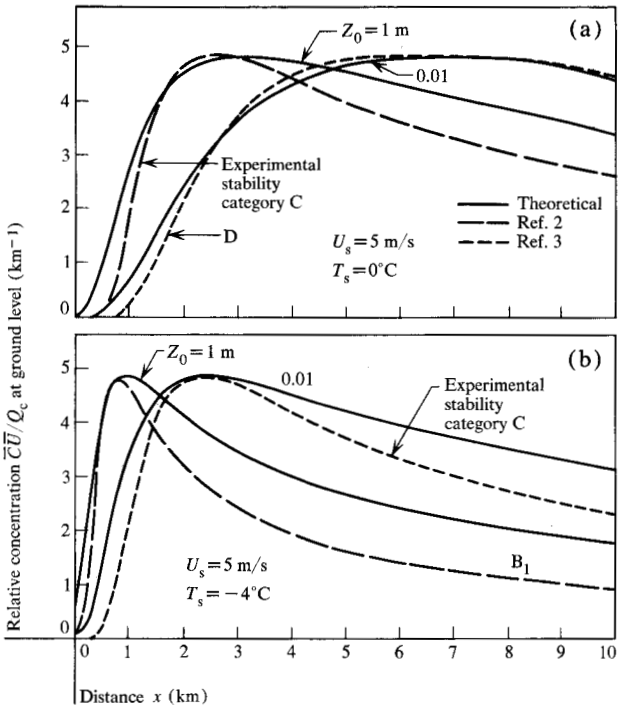

Figure 4 Comparison of theoretical and experimental ground-level concentration distributions for (a) neutrally stable and (b) unstable atmospheric conditions.

for neutral stability. We see that the greater the ground roughness, the larger the eddy diffusivity. The eddy diffusivity increases with height from the ground and reaches its maximum value near 300 m. It then decreases to the top of the layer. In Fig. 2(b) the wind profile is seen to become more nonuniform with increasing ground roughness, due to intensified mixing.

The ground-level pollutant concentration in terms of the relative concentration $\overline{C}\overline{U}/Q_c$ is shown in Fig. 3. The location of the maximum concentration is closer to the stack for larger ground roughness, and the magnitude of the maximum increases with increasing roughness. This is qualitatively different from the results for a Gaussian plume. If the plume were Gaussian, the maximum value would be $(2/\pi e)^{1/2}/h_s$, according to Eq. (34). In Fig. 3, however, the maximum value is greater than this. The difference arises because the wind field is more nonuniform for larger Z_0, causing the plume distribution to differ from Gaussian, which is based on a uniform-wind assumption.

In Fig. 4(a) we compare our numerical results with experiments. Two sets of experimental data were chosen; one set is known as the Pasquill-Gifford data[3], the other is from Brookhaven National Laboratory[2]. The comparison shows fair agreement between Brookhaven data and the present computation with $Z_0 = 1$ m, and the Pasquill-Gifford data is close to the curve for $Z_0 = 0.01$ m. Ground roughness at the Brookhaven test site is about 1 m (I. A. Singer, personal communication). Pasquill's data, restated by Gifford, are apparently taken from Prairie Grass data with ground roughness about 0.6 cm[9]. This suggests that the apparent inconsistency between the two sets of data is due to differing ground roughness. A similar conclusion follows from Fig. 4(b) for an unstable atmosphere in which Pasquill's stability category C and Brookhaven's category B_1 have been chosen for comparison.

In Figs. 4(a) and 4(b) the numerical values are larger than experimental values at distances far downwind. One of the reasons may be that the vertical variation of the wind direction causes the plume center line to vary downwind and thus tilts the cross section of the plume at large distances. Consequently, the ground-level concentration in a straight downwind direction from the stack decreases with increasing deviation of the wind direction. This effect has been described by Michael[10]. On the other hand, accurate measurements of pollutant concentration, meteorological factors, and ground conditions are more difficult to obtain far from the stack.

Differences between the numerical results and the observations near the stack may be due to inadequate resolution of the finite difference scheme. Near the stack the cross section of the plume is smaller than the grid size and the concentration has sharp variations across the plume. Another cause of this difference near the stack might be the assumption that $K_c = K_c(z) \neq K_c(x,z)$.

The real point of interest is the location of the *maximum* ground-level concentration. For a stable atmosphere, the locations of the maximum concentrations for

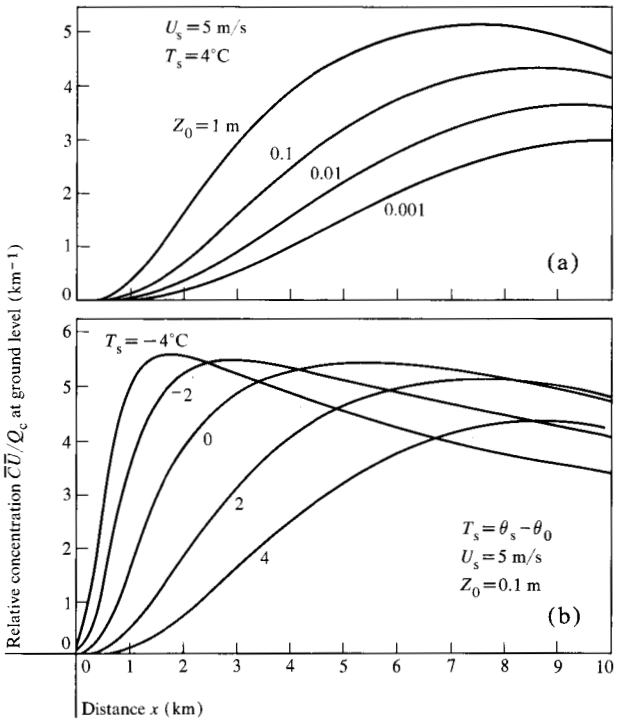

Figure 5 Variation of relative ground-level pollutant concentration with (a) ground roughness and (b) atmospheric stability.

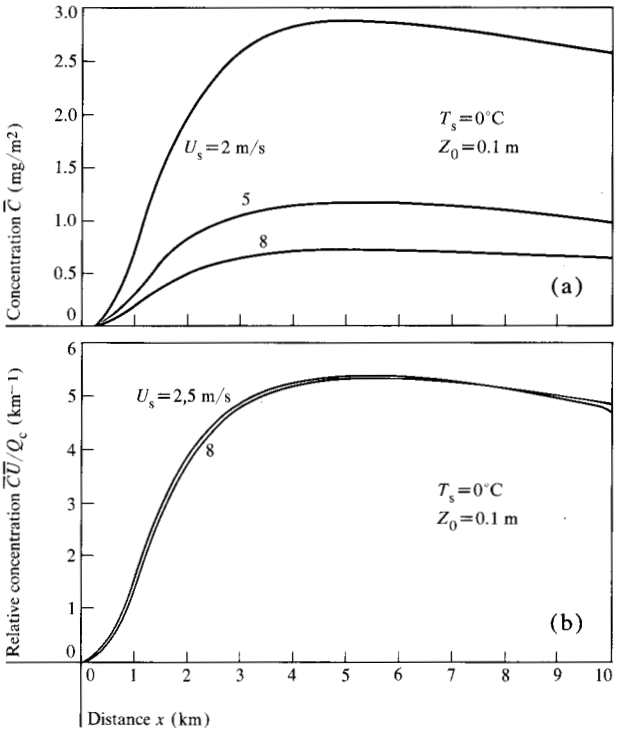

Figure 7 Horizontal variation of (a) actual and (b) relative ground-level pollutant concentrations with wind speed at stack height.

Figure 6 Vertical variation of wind speed with wind speed at stack height.

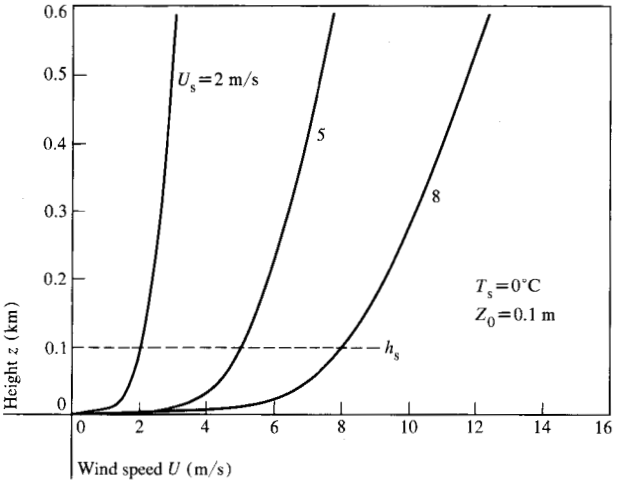

different values of Z_0 [Fig. 5(a)] are spread wider at greater distances downstream. The comparison with experiments is difficult because no clear relation exists between the stability category used in experiments and the stability parameter used in theory.

•• *Atmospheric stability*

The influence of atmospheric stability on ground-level pollutant concentration is shown in Fig. 5(b). The location of the maximum concentration is close to the stack for the unstable case and moves away as stability increases. We did not compute the extremely stable and unstable cases, because it is not clear whether the formulas (7) and (15) are valid in such cases.

•• *Wind speed*

For the neutrally stable case with $Z_0 = 0.1$ m, wind speeds at stack height were chosen as 2, 5, and 8 m/s. These values provide the velocity profiles shown in Fig. 6. The ground-level pollutant concentration is shown in Fig. 7(a), the magnitude being inversely proportional to wind speed. The relative ground-level concentration is shown in Fig. 7(b). The effect of the wind speed is obviously negligible in this (neutral atmospheric stability) case.

•• *Effective mean wind*

The effective mean wind defined by Eq. (35) has been regarded as monotonically increasing downwind from the stack. In Fig. 8(a) the effective mean wind decreases to a minimum at a certain distance from the stack and then in-